Journal of Zhejiang University-SCIENCE A (Applied Physics & Engineering)
ISSN 1673-565X (Print); ISSN 1862-1775 (Online)
www.zju.edu.cn/jzus; www.springerlink.com
E-mail: jzus@zju.edu.cn

Influence of ash composition on the sintering behavior during pressurized combustion and gasification process*

Ni-jie JING, Qin-hui WANG†‡, Yu-kun YANG, Le-ming CHENG, Zhong-yang LUO, Ke-fa CEN

(*State Key Laboratory of Clean Energy Utilization, Zhejiang University, Hangzhou 310027, China*)

†E-mail: qhwang@zju.edu.cn

Received Aug. 4, 2011; Revision accepted Oct. 27, 2011; Crosschecked Feb. 7, 2012

Abstract: To determine the ash characteristics during fluidized bed combustion and gasification purposes, the investigation of the impacts of chemical composition of Jincheng coal ash on the sintering temperature was conducted. A series of experiments on the sintering behavior at 0.5 MPa was performed using the pressurized pressure-drop technique in the combustion and gasification atmospheres. Meanwhile, the mineral transformations of sintered ash pellets were observed using X-ray diffractometer (XRD) analyzer to better understand the experimental results. In addition, quantitative XRD and field emission scanning electron microscope/energy dispersive X-ray spectrometer (FE-SEM/EDS) analyses of ash samples were used for clarifying the detailed ash melting mechanism. These results show that the addition of Fe_2O_3 can obviously reduce the sintering temperatures under gasification atmospheres, and only affect a little the sintering temperature under combustion atmosphere. This may be due to the presence of iron-bearing minerals, which will react with other ash compositions to produce low-melting-point eutectics. The FE-SEM/EDS analyses of ash samples with Fe_2O_3 additive show consistent results with the XRD measurements. The CaO and Na_2O can reduce the sintering temperatures under both the combustion and gasification atmospheres. This can be also contributed to the formation of low-melting-point eutectics, decreasing the sintering temperature. Moreover, the fluxing minerals, such as magnetite, anhydrite, muscovite, albite and nepheline, contribute mostly to the reduction of the sintering temperature while the feldspar minerals, such as anorthite, gehlenite and sanidine, can react with other minerals to produce low-melting-point eutectics, and thereby reduce the sintering temperatures.

Key words: Ash composition, Sintering temperature, X-ray diffractometer (XRD), Field emission scanning electron microscope/energy dispersive X-ray spectrometer (FE-SEM/EDS)

doi:10.1631/jzus.A1100206 **Document code:** A **CLC number:** TQ533

1 Introduction

The coal combustion and gasification as efficient and clean coal utilization technologies have been paid much attention and are widely used in many fields, including gas production and synthetic chemicals. However, ash-related operational problems are usually found in these combustion and gasification technologies (Wu *et al*., 2000; Ishom *et al*., 2002). These problems are bed agglomeration, bridging on hot gas filtration systems, and deposition on heat exchanger tubes and gas circuits as a result of ash build-up (Al-Otoom *et al*., 2000a; 2000b; Ishom *et al*., 2002), which can reduce the thermal economics of the system and even affect the stability of the system. The investigations show that the formation of melts and sinters of coal ash should be responsible for the above-mentioned problems. Also, the present studies indicate that the sintering of coal ash is one of the dominant mechanisms of these problems in the fluidized beds, and hence, it is necessary to investigate the sintering characteristics of coal ash for the continued operation of fluidized bed combustion and gasification system.

Conversely, as ash properties change with the

‡ Corresponding author

* Project (No. 2011DFA72730-202) supported by the Research Project of US-China Clean Energy Research Center

composition, the melting and sintering properties of coal ash also vary considerably. Hence, the sintering behavior is related to the chemical composition of coal ash. Various studies discussed that the agglomeration of bed particles in atmospheric fluidized bed combustion systems utilizing black coal has been attributed to the sintering of the product of the reaction between CaO and SO_2 or CO_2 (Dawes *et al*., 1988; Skrifvars *et al*., 1992; 1994). Lolja *et al*. (2002) presented an analysis of the ash fusion temperatures (AFTs) for 17 Albanian coals and investigated the contribution of oxides to AFTs by considering oxides from various perspectives such as discrete species, acids and bases, crystal components, fluxing agents, and cement constituents. Alpern *et al*. (1984), Seggiani (1999) and Song *et al*. (2010) reported the fusibility of the ash as function of the content of the principal oxides frequently found in coal ash, i.e., SiO_2, Fe_2O_3, CaO, MgO, etc. However, only limited studies have been undertaken on sintering behavior as the function of ash chemical composition under pressurized conditions.

In addition, the sintering behavior of coal ash has been determined using a number of techniques, such as the compressive strength method, the electrical conductance technique, the dilatometer and thermo-mechanical analysis (Gupta *et al*., 1998; Al-Otoom *et al*., 2000a). In this study, an improved new technique (pressurized pressure-drop technique) is considered to determine the sintering temperature of coal ash by measuring the pressure-drop across an ash pellet. The purpose of this paper is to explore the relationship between the sintering behavior and chemical composition and minerals of coal ash using the pressurized pressure-drop technique, X-ray diffractometer (XRD) and field emission scanning electron microscope/energy dispersive X-ray spectrometer (FE-SEM/EDS) analyses at 0.5 MPa. By evaluating these relationships, a reliable explanation and a detailed understanding can be made concerning the sintering behavior of the inorganic matter during pressurized process.

2 Experimental

Experiments were performed for investigating the sintering behavior during the pressurized combustion and gasification process. In order to model a realistic environment and make a comparison, the simulated combustion and gasification atmospheres have been used for this study. The gas compositions of the simulated atmospheres of mixed gases are shown in Table 1.

Table 1 Gas compositions (in volume) of the simulated atmospheres of mixed gases

Atmosphere	Gas composition (%)					
	H_2	CH_4	CO	CO_2	O_2	N_2
Combustion				49.7	2.1	48.2
Gasification	40.8	1.9	36.5	20.8		

2.1 Preparation of samples

The Chinese Jincheng coal samples have been characterized recently (Jing *et al*., 2012) and its ash chemical composition is shown in Table 2. Briefly, the ash samples produced from the laboratory have been mixed into the pure chemical reagents (Fe_2O_3, CaO and Na_2CO_3). Then, the mixtures were heated to 815 °C for 1 h and then different proportion samples were obtained. Finally, the samples were ground in a mortar to a particle size <200 μm for homogeneous mixing.

Table 2 Ash chemical composition of the coal

Composition	Value (%)	Composition	Value (%)
SiO_2	48.10	Na_2O	1.14
Al_2O_3	31.84	K_2O	1.09
Fe_2O_3	5.90	MgO	0.98
CaO	4.96	SO_3	3.07

2.2 Ash sintering characteristic measurements

A schematic diagram of the pressurized pressure-drop measuring device is shown in Fig. 1. The setup consists of a high temperature tube furnace fitted with a temperature controller, a gas system, a measurement system and a shell. In this experiment, N_2 gas (purity: 99.999%) was used to maintain the desired pressure in the shell. The detail of this setup refers to the previous report (Jing *et al*., 2012).

Whilst the sintering process occurs, the pellet starts to shrink, and thus pulls away from the wall of the quartz tube, resulting in the formation of new pathways for the passage of air (Al-Otoom *et al*., 2000a). Thus, there will be a marked pressure-drop decrease. The sintering temperature is designated as the point where the pressure-drop becomes a maximum. The technique of measuring pressure-drop is a

new measurement with reproducibility of ±9 °C, which is obtained by repeating at least twice using at least two samples from the same batch, and is in accordance with the literature (Delvinquier *et al*., 1995; Al-Otoom *et al*., 2000a).

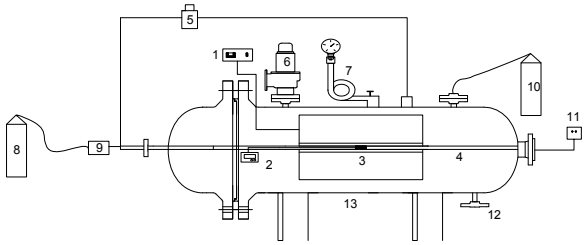

1: temperature controller; 2: measured temperature thermocouple; 3: tube furnace; 4: quartz tube; 5: pressure-drop transmitter; 6: safety valve; 7: pressure gauge; 8: reaction gas cylinder; 9: mass flow meter; 10: pressurized gas cylinder; 11: thermal resistance; 12: pressure-release valve; 13: shell

Fig. 1 Experimental device of pressurized pressure-drop technique (Jing *et al*., 2012)

2.3 Analytical techniques

The sintered samples were ground in a mortar to a particle size <74 μm and then scanned using a Rigaku D/Max-2550PC XRD. The accelerating voltage was 40 kV and the current was 250 mA. X-ray diffraction traces were made using a diffractometer with copper Kα radiation at (5°–85°)/(2θ) at a scan rate of 10°/min. XRD data were obtained by measuring the relative intensities of the characteristic diffraction peaks for identified minerals in the XRD patterns. This measurement method assumes that the ratio of the peak heights is relatively proportional to the mineral concentrations (Vassilev *et al*., 1995; Yang *et al*., 2009).

In addition, the quantitative XRD analyses of ash samples with 10% and 35% Fe_2O_3 additions under the gasification atmosphere were performed. X-ray diffraction traces were also made using a Rigaku D/Max-2550pc powder diffractometer with copper Kα (λ for Kα is 0.154059 nm) radiation at 40 kV and 250 mA. The scans were run from (5°–90°)/(2θ), with an increasing step size of 0.02°/s.

A field emission scanning electron microscope (FE-SEM) (SIRION-100, FEI) was used to examine the surface morphology change of ash samples with 10% and 35% Fe_2O_3 under the combustion atmosphere. The qualitative element identification and semiquantitative analysis of ash samples were obtained by using the EDAX GENESIS4000 EDS system (USA). The EDS analyses were performed on particle samples by operating FE-SEM at an accelerating voltage of 25 kV. The intensity ratios of various constituent elements present in EDS spectra were also used to identify the chemical composition of partial melting parts in ash.

3 Results and discussion

3.1 Effect of Fe_2O_3 on the sintering temperature

The effect of Fe_2O_3-content on the sintering temperatures at 0.5 MPa is given in Fig. 2. From Fig. 2, the sintering temperature falls obviously under the gasification atmosphere. This result is consistent with investigations into the atmospheric pressure. The main reason is that Fe_2O_3 can be converted into FeO in the gasification atmosphere (McLennan *et al*., 2000; Li *et al*., 2009), and the Fe(II) may react with the CaO, SiO_2 and Al_2O_3 to produce low-temperature eutectics and form the liquid phases (Sheng and Li, 2008; van Dyk *et al*., 2009; Song *et al*., 2009a), and thereby decreasing the sintering temperatures. Therefore, the sintering temperature decreases as the Fe_2O_3 content increases under the gasification atmosphere.

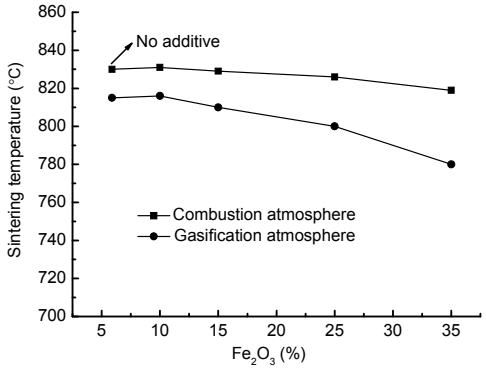

Fig. 2 Effect of Fe_2O_3 on the sintering temperature at 0.5 MPa

Conversely, the sintering temperature changes only a little with the Fe_2O_3-content under the combustion atmosphere. This is because iron highly accelerates the formation of polymer and increases slag viscosity when it is present as Fe(III) under the combustion atmosphere (ten Brink *et al*., 1996), and thus increasing the sintering temperature. However,

only the part of Fe(II) promotes the fluxing of slag. Hence, the decrease degree is a little smaller with the increase in Fe_2O_3 under the combustion atmosphere.

Compared with previous results performed under combustion and gasification conditions at atmospheric pressure (Wang *et al*., 2010; Jing *et al*., 2012), the degree decrease of sintering temperature is not obvious at the higher pressure (0.5 MPa). This may be that increasing pressure will lead to an increase in gas viscosity and density directly (Wall *et al*., 2002) which then affects the reaction gas pulling away from the wall of the quartz tube (namely, the sintering process). Furthermore, the dependence of reaction rate on pressure decreases with increasing pressure (Wall *et al*., 2002). Therefore, the chemical reaction rates in the ash may be lowered at high pressure. Thus, high pressure influence on the sintering temperature is weakened.

Furthermore, Figs. 3a and 3b presents the XRD patterns of 0.5 MPa ash samples under the combustion and gasification atmospheres. The results show

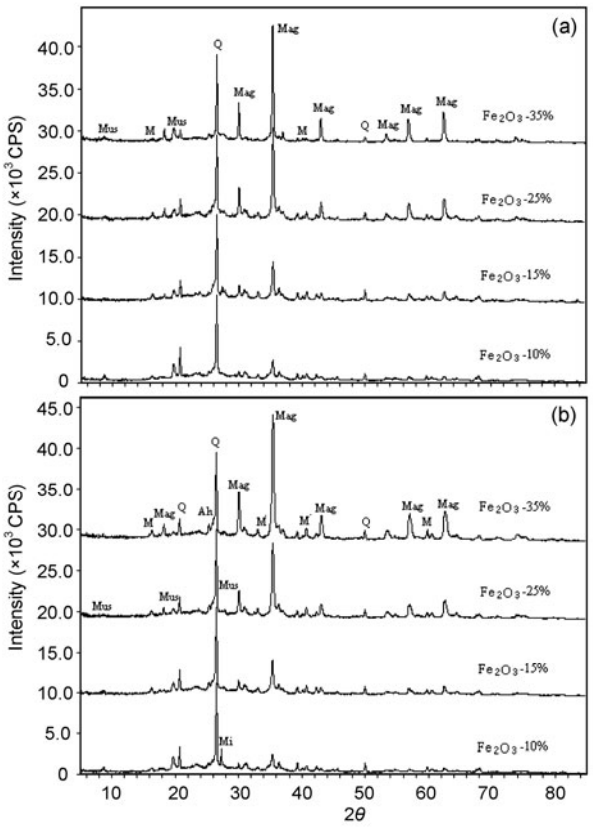

Fig. 3 XRD patterns under combustion (a) and gasification (b) atmospheres with different Fe_2O_3 additions
Q: quartz; Mag: magnetite; Ah: anhydrite; Mi: microcline; Mus: muscovite; M: mullite

that the main minerals are quartz, magnetite, muscovite ($KAl_2(Al{\cdot}Si_3O_{10})(OH)_2$) and mullite ($Al_6Si_2O_{13}$) under the combustion atmosphere. By increasing Fe_2O_3 to 25%, the magnetite increases; while the peak of muscovite, as a fluxing mineral (Bryant *et al*., 1998; Vassileva and Vassilev, 2006), decreases. Hence, the extent of the decrease of sintering temperature is not obvious in the combustion atmosphere.

Conversely, under the gasification atmosphere, anhydrite and microcline are also detected apart from quartz, mullite, muscovite and magnetite. With the addition of Fe_2O_3, the muscovite and microcline decompose and melt gradually, whilst the diffraction peak intensity of anhydrite increases. Microcline, muscovite and anhydrite are fluxing minerals (Bryant *et al*., 1998; Vassileva and Vassilev, 2006). The presence of these minerals results in the lower sintering temperatures under the gasification atmosphere. In addition, the magnetite as a fluxing mineral increases obviously with the increase in Fe_2O_3, and thus leads to a dramatic drop of the sintering temperature.

To clarify the detailed ash melting mechanism, the chemical and textural variations of ash sample with 10% and 35% Fe_2O_3 under combustion atmosphere were examined using FE-SEM/EDS. The mineral proportions in coal ash with Fe_2O_3 addition in the gasification atmosphere were performed by using a quantitative X-ray diffraction analyzer.

As shown in Fig. 4, the nonspherical aluminosilicate minerals with Fe, K and Na are detected to melt partly at 10% Fe_2O_3 (Figs. 4a–4d). The degree of ash melting gradually increased with the increasing Fe_2O_3 (Figs. 4e–4h). The chemical compositions of ash samples with 10% and 35% Fe_2O_3 under the combustion atmosphere were obtained by EDS (Table 3). Along with the proceeding of Fe_2O_3, the fraction of Fe shows an increased concentration and the fractions of K and Na decrease (Figs. 4d and 4h). This indicates that K(Na)-containing minerals may melt and decrease. This result is in accordance with the XRD pattern.

Table 3 Main elements of samples under the combustion atmosphere

Addition	Element composition (%)						
	Si	Al	Fe	Ca	K	Na	Mg
10% Fe_2O_3	25.94	18.13	6.16	2.90	1.40	1.21	0.99
35% Fe_2O_3	18.34	14.09	27.54	2.24	1.06	0.86	0.63

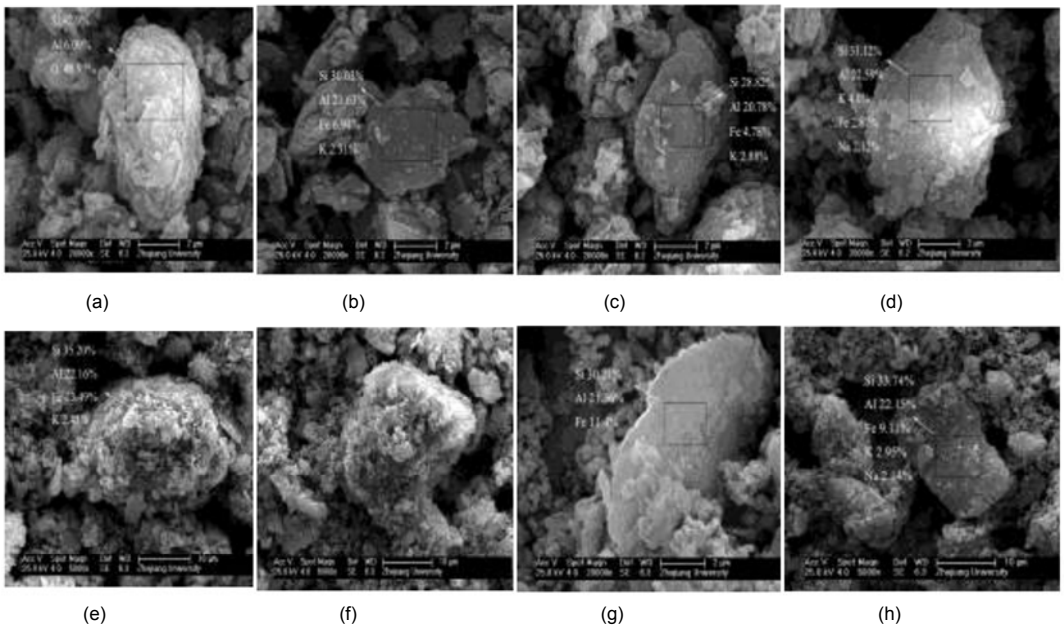

Fig. 4 FE-SEM micrographs of ash samples with 10% and 35% Fe_2O_3 under combustion atmosphere
(a)–(d) ash samples with 10% Fe_2O_3 with high contents of K and Na; (e)–(f) ash samples with 35% Fe_2O_3 with high content of Fe

Table 4 gives the quantitative X-ray diffraction results of coal ash with Fe_2O_3 addition under the gasification atmosphere. The addition of Fe_2O_3 to the coal ash is reflected in the presence of magnetite. Simultaneously, the anhydrite and mullite increase while the muscovite is dramatically decreased with the addition of Fe_2O_3, suggesting that the addition of Fe_2O_3 may facilitate the fusion of low-melting-point mineral, thereby reducing the sintering temperature. Also, the fluxing minerals, such as magnetite and anhydrite, decrease the sintering temperature. This finding is consistent with the above qualitative results under the gasification atmosphere.

Table 4 Mineral proportions in coal ash with Fe_2O_3 addition in the gasification atmosphere

Addition	Mineral proportion				
	SiO_2	Fe_3O_4	$Al_6Si_2O_{13}$	$CaSO_4$	$KAl_2(Al{\cdot}Si_3O_{10})(OH)_2$
10% Fe_2O_3	31.9	5.6	30.5	0.5	31.4
35% Fe_2O_3	19.4	37.5	39.5	3.7	0

3.2 Effect of CaO on the sintering temperature

Fig. 5 is a plot of sintering temperatures against CaO content in different reaction atmospheres. As shown in Fig. 5, the sintering temperatures decrease under both the combustion and gasification atmospheres as the CaO content increases. Again, this is consistent with previous work performed at atmospheric pressure. Song *et al*. (2009b) and Ninomiya and Sato (1997) presented that the fusion temperatures of ash decrease as CaO content increases. Also, Cen *et al*. (1994) studied the viscosity curve trend with the CaO-content, and showed that the viscosity of the coal ash decreases as the CaO content increases, thereby leading to the reduction in the sintering temperature.

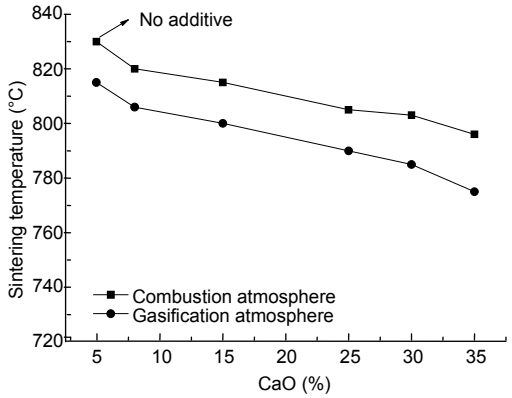

Fig. 5 Effect of the CaO on the sintering temperature at 0.5 MPa

From the XRD results in Fig. 6a, under the combustion atmosphere, it can be seen that the mullite

disappears while the sanidine ($(K,Na)(Si,Al)_4O_8$) transforms into anorthite ($CaO{\cdot}Al_2O_3{\cdot}2SiO_2$) from 8% to 15% CaO. Also, the andradite ($Ca_3Fe_2Si_3O_{12}$) is detected. This may be due to the reaction of albite ($NaAlSi_3O_8$), anorthite and iron-bearing minerals. With the increase of CaO, a peak of gehletite ($2CaO{\cdot}Al_2O_3{\cdot}SiO_2$) is observed and the magnetite transforms into hematite. The gehlenite, formed as reaction products from anhydrite, alumina and silica at temperatures around 900 °C and also formed directly from lime (van Dyk *et al*., 2008), can react with other minerals to produce the low temperature eutectics, leading to the decrease of the sintering temperature. In addition, the presence of albite, andradite and anorthite also lead to the lower sintering temperature.

Under the gasification atmosphere (Fig. 6b), with an increase in CaO, the peaks of mullite and magnetite disappear. This indicates that mullite decomposes and magnetite melts into glass phase. From 25% to 30% CaO, the albite transforms into microcline. The microcline can reduce the sintering temperature. Also, the peaks of muscovite and gehlenite increase with the addition of CaO. Muscovite as a fluxing mineral can also reduce the sintering temperatures. Furthermore, the feldspar minerals, such as albite, anorthite and gehlenite, can react with other minerals to generate the low temperature eutectics, thereby decreasing the sintering temperature.

Therefore, the sintering temperature decreases with increasing CaO-content under both the combustion and gasification atmospheres. Similarly, the sintering temperatures under the gasification atmosphere are lower than those under the combustion atmosphere. Moreover, the degree decrease of sintering temperature at the higher pressure (0.5 MPa) is also smaller than at atmospheric pressure.

3.3 Effect of Na_2O on the sintering temperature

Fig. 7 indicates that the sintering temperatures are decreasing with the increase in Na_2O contents under both the combustion and gasification atmospheres. Also, the Na_2O content significantly affects the sintering temperature. The reason may be that sodium as a modifier of network is an efficient fusion agent and is easy to crystallize with SiO_2. With the increase of the addition of sodium, it breaks some of the oxygen bonds that provide structure to the clay minerals, resulting in a low melting temperature (Swanson, 2000; Li *et al*., 2010). In addition, according to Cen *et al*. (1994), Na_2O will react with other minerals to produce low temperature eutectics, causing the decrease of the sintering temperature.

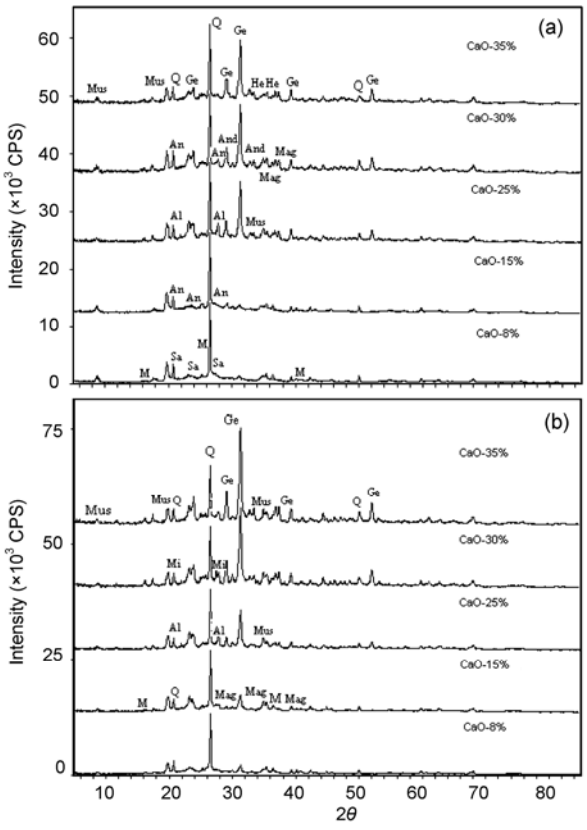

Fig. 6 XRD patterns under combustion (a) and gasification (b) atmospheres with different CaO additions
Q: quartz; Mag: magnetite; An: anorthite; And: andradite: Al: albite; He: hematite; Ge: gehlenite; Mus: muscovite; Mi: microcline; M: mullite

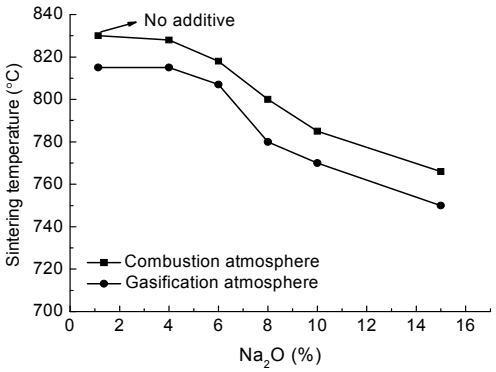

Fig. 7 Effect of the Na_2O on the sintering temperature at 0.5 MPa

Fig. 8 shows the XRD patterns of 0.5 MPa ash samples with different Na_2O contents. It can be seen that fluxing minerals do exist with the increase in Na_2O-content.

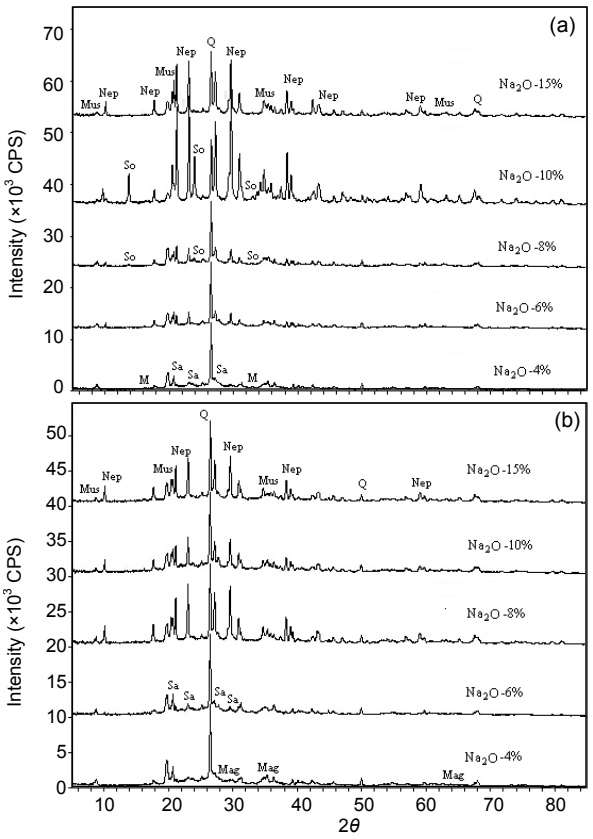

Fig. 8 XRD patterns under combustion (a) and gasification (b) atmospheres with different Na_2O additions
Q: quartz; Mag: magnetite; Sa: sanidine; So: sodalite; Mus: muscovite; Nep: nepheline

Under the combustion atmosphere, there are quartz, sanidine, mullite and muscovite at 4% Na_2O. The phases of mullite and sanidine disappear and a peak of nepheline ($NaAlSiO_4$) appears at 6% Na_2O. Sodalite ($Na_8Al_6Si_6O_{24}Cl_2$) is observed at 8% Na_2O, which is a member of the feldspathoid mineral group and whose chemical property is close to that of the alkali feldspars but is poor in silica (SiO_2) content. When Na_2O is further added to 10%, the intensities of sodalite, nepheline and muscovite reach their maximum. Hence, the extent of decrease of sintering temperature shows most at 10% Na_2O. When the Na_2O content reaches 15%, the sodalite disappears. This may be that sodalite begins to decompose and transform into nepheline, which is a typical basic mineral with low fusibility, and can reduce the sintering temperature. The presence of these fluxing minerals could explain why the addition of Na_2O reduces the sintering temperature.

Under the gasification atmosphere, when the Na_2O content reaches 6%, a sanidine peak is observed and the magnetite peak disappears. This suggests that the magnetite may melt into glass, which is low melting (Brooker and Oh, 1995) and not detected by XRD. At 8% Na_2O, nepheline is present and thus obviously leads to the decrease of sintering temperature. Also, this trend can be seen from Fig. 7. The peak of nepheline shows highest at 8% Na_2O. This may be due to the transformation from other minerals and sufficient reactions of forming nepheline. The further formation of nepheline results in the decrease of the sintering temperature.

In general, as the Na_2O increases, many fluxing minerals, such as magnetite, sodalite and nepheline (Vassileva and Vassilev, 2006), are present, which can dramatically decrease the sintering temperature, especially the nepheline. Therefore, the sintering temperatures are decreasing with the increase in Na_2O-contents under both the combustion and gasification atmospheres.

Similarly, the degree decrease of sintering temperature at the higher pressure (0.5 MPa) is also smaller than the results at atmospheric pressure.

In addition, the calculations for the FeO-CaO-SiO_2-Al_2O_3-Na_2O five-component system using FactSage have been conducted in (Jing *et al*., 2012). There are fayalite ($2FeO{\cdot}SiO_2$), hercynite ($FeO{\cdot}Al_2O_3$), ferrocordierite ($2FeO{\cdot}2Al_2O_3{\cdot}5SiO_2$), Fe-akermanite ($2CaO{\cdot}FeO{\cdot}2SiO_2$), rankinite ($3CaO{\cdot}SiO_2$), Ca_2SiO_4 ($2CaO{\cdot}SiO_2$), $CaSiO_3$, gehlenite, anorthite, and sodium silicate in the five-component system. The sodium-calcium silicate and SiO_2 can produce low temperature common-fluxing minerals at temperatures as low as 725 °C. Also, the fayalite, hercynite and calcium-containing minerals can produce low-melting minerals, according to the phase diagram. These low temperature common-melting minerals can reduce the sintering temperature. Therefore, the calculation results are consistent with the experiment data.

4 Conclusions

Series of experiments and analyses have been conducted by using a pressurized pressure-drop measurement setup and the XRD. In addition, the quantitative XRD and FE-SEM/EDS analyses of ash samples have also been performed for further clarifying the detailed ash melting mechanism. It can be concluded as follows.

1. The sintering temperatures under the gasification atmosphere are lower than that under the combustion atmosphere and this presents a similar trend, compared to the atmospheric condition, but the extent of decrease is a little smaller at higher pressure.

2. The additive of Fe_2O_3 can obviously reduce the sintering temperatures under the gasification atmospheres, and affect only a little the sintering temperature under the combustion atmosphere. This can be due to the presence of iron-containing and fluxing minerals from the XRD results, such as the magnetite, anhydrite, muscovite and microcline, leading to the decrease in sintering temperature. In addition, the FE-SEM/EDS analyses suggest that the nonspherical aluminosilicate minerals with Fe, K or Na are found to melt. This finding is in accordance with the XRD results.

3. The CaO and Na_2O can reduce the sintering temperatures under both the combustion and the gasification atmospheres. This can be contributed to the formation of low temperature eutectics. With the increasing CaO, there are fluxing minerals (anhydrite, and microcline) and some feldspar minerals, such as albite, anorthite and gehlenite, easy to produce low-temperature eutectics with other minerals, and thereby declining the sintering temperature. Conversely, with the increase in Na_2O, the fluxing minerals, such as muscovite, nepheline and sodalite, lead to the reduction of the sintering temperature.

4. The XRD and FE-SEM/EDS patterns showed that the sintering temperature change of ash is mainly caused by chemical composition and mineral composition. Also, the presence of fluxing minerals (magnetite, anhydrite, muscovite, and nepheline) contributes mostly for the decrease of the sintering temperature. Meanwhile, the feldspar minerals, such as albite, anorthite, gehlenite and sanidine, can produce low temperature eutectics, which decrease the sintering temperatures.

References

Al-Otoom, A.Y., Bryant, G.W., Elliott, L.K., Skrifvars, B.J., Hupa, M., Wall, T.F., 2000a. Experimental options for determining the temperature for the onset of sintering of coal ash. *Energy & Fuels*, **14**(1):227-233. [doi:10.1021/ef990196s]

Al-Otoom, A.Y., Elliott, L.K., Wall, T.F., Moghtaderi, B., 2000b. Measurement of the sintering kinetics of coal ash. *Energy & Fuels*, **14**(5):994-1001. [doi:10.1021/ef0000126]

Brooker, D.D., Oh, M.S., 1995. Iron sulfide deposition during coal gasification. *Fuel Processing Technology*, **44**(1-3):181-190. [doi:10.1016/0378-3820(95)00011-U]

Bryant, G.W., Lucas, J.A., Gupta, S.K., Wall, T.F., 1998. Use of thermomechanical analysis to quantify the flux additions necessary for slag flow in slagging gasifiers fired with coal. *Energy & Fuels*, **12**(2):257-261. [doi:10.1021/ef9700846]

Cen, K.F., Fan, J.R., Chi, Z.H., 1994. Mechanisms and Calculations for Preventing Boilers and Heat Exchangers from Depositing, Slagging, Wearing and Eroding. Science Press, Beijing, China (in Chinese).

Dawes, S.G., Gibbs, G.B., Highley, H., 1988. The British coal/CEGB project on pressurised fluidised bed combustion. *Journal of Institute of Energy*, **17**:17-26.

Delvinquier, V., Fatah, N., Pietrzyk, S., Dauphin, J., Berte, P., Bruyet, B., 1995. Defluidisation at High Temperature in Fluidised Bed of Sand by Addition of Calcium Carbonate. Fluidised Bed Combustion, Heinschel, K.J. (Ed.), ASME, New York, **2**:801-806.

Gupta, S.K., Gupta, R.P., Bryant, G.W., Wall, T.F., 1998. The effect of potassium on the fusibility of coal ashes with high silica and alumina levels. *Fuel*, **77**(11):1195-1201. [doi:10.1016/S0016-2361(98)00016-7]

Ishom, F., Harada, T., Aoyagi, T., Sakanishi, K., Korai, Y., 2002. Problem in PFBC boiler (1): characterization of agglomerate recovered in commercial PFBC boiler. *Fuel*, **81**(11-12):1146-1148. [doi:10.1016/S0016-2361(02)00066-2]

Jing, N.J., Wang, Q.H., Luo, Z.Y., Cen, K.F., 2012. Effect of the chemical composition on the sintering behavior of Jincheng coal ash under the gasification atmosphere. *Chemical Engineering Communications*, **199**(2):189-202. [doi:10.1039/c1cc12040a]

Li, J.B., Shen, B.X., Li, H.X., Zhao, J.G., Wang, J.M., 2009. Effect of ferrum-based flux on the melting characteristics of coal ash from coal blends using the Liu-qiao No. 2 Coal Mine in Wan-bei. *Journal of Fuel Chemistry and Technology*, **37**(3):262-265. [doi:10.1016/S1872-5813(09)60020-7]

Li, W.D., Li, M., Li, W.F., Liu, H.F., 2010. Study on the ash fusion temperatures of coal and sewage sludge mixtures. *Fuel*, **89**:1566-1572. [doi:10.1016/j.fuel.2009.06.031]

Lolja, S.A., Haxhi, H., Dhimitri, R., Drushku, S., Malja, A., 2002. Correlation between ash fusion temperatures and chemical composition in Albanian coal ashes. *Fuel*, **81**(17):2257-2261. [doi:10.1016/S0016-2361(02)00194-1]

McLennan, A.R., Bryant, G.W., Stanmore, B.R., Wall, T.F., 2000. Ash formation mechanisms during pf combustion in reducing conditions. *Energy & Fuels*, **14**(1):150-159. [doi:10.1021/ef990095u]

Ninomiya, Y., Sato, A., 1997. Ash melting behavior under coal gasification conditions. *Energy Conversion and Management*, **38**(10-13):1405-1412. [doi:10.1016/S0196-8904(96)00170-7]

Seggiani, M., 1999. Empirical correlations of the ash fusion temperatures and temperature of critical viscosity for coal and biomass ashes. *Fuel*, **78**(9):1121-1125. [doi:10.1016/S0016-2361(99)00031-9]

Sheng, C.D., Li, Y., 2008. Experimental study of ash formation during pulverized coal combustion in O_2/CO_2 mixtures. *Fuel*, **87**(7):1297-1305. [doi:10.1016/j.fuel.2007.07.023]

Skrifvars, B.J., Hupa, M., HiItunen, M., 1992. Sintering of ash during fluidized bed combustion. *Industrial & Engineering Chemistry Research*, **31**(4):1026-1030. [doi:10.1021/ie00004a008]

Skrifvars, B.J., Hupa, M., Backman, R., HiItunen, M., 1994. Sintering mechanisms of FBC ashes. *Fuel*, **73**(2):171-176. [doi:10.1016/0016-2361(94)90110-4]

Song, W.J., Tang, L.H., Zhu, X.D., Wu, Y.Q., Rong, Y.Q., Zhu, Z.B., Koyama, S., 2009a. Fusibility and flow properties of coal ash and slag. *Fuel*, **88**(2):297-304. [doi:10.1016/j.fuel.2008.09.015]

Song, W.J., Tang, L.H., Zhu, X.D., Wu, Y.Q., Zhu, Z.B., Koyama, S., 2009b. Prediction of Chinese coal ash fusion temperatures in Ar and H_2 atmospheres. *Energy & Fuels*, **23**:1990-1997. [doi:10.1021/ef800974d]

Song, W.J., Tang, L.H., Zhu, X.D., Wu, Y.Q., Zhu, Z.B., Koyama, S., 2010. Effect of coal ash composition on ash fusion temperatures. *Energy & Fuels*, **24**(1):182-189. [doi:10.1021/ef900537m]

Swanson, M.L., 2000. Modeling of Ash Properties in Advanced Coal-Based Power System. Grand Forks, North Dakota.

ten Brink, H.M., Eenkhoorn, S., Hamburg, G., 1996. A mechanistic study of the formation of slags from iron-rich coals. *Fuel*, **75**(8):952-958. [doi:10.1016/0016-2361(96)00048-8]

van Dyk, J.C., Waanders, F.B., Hack, K., 2008. Behaviour of calcium-containing minerals in the mechanism towards in situ CO_2 capture during gasification. *Fuel*, **87**(12):2388-2393. [doi:10.1016/j.fuel.2008.03.015]

van Dyk, J.C., Benson, S.A., Laumb, M.L., Waanders, B., 2009. Coal and coal ash characteristics to understand mineral transformations and slag formation. *Fuel*, **88**(6):1057-1063. [doi:10.1016/j.fuel.2008.11.034]

Vassilev, S.V., Kitanob, K., Takedab, S., Tsurueb, T., 1995. Influence of mineral and chemical composition of coal ashes on their fusibility. *Fuel Processing Technology*, **45**(1):27-51. [doi:10.1016/0378-3820(95)00032-3]

Vassileva, C.G., Vassilev, S.V., 2006. Behaviour of inorganic matter during heating of Bulgarian coals 2. Subbituminous and bituminous coals. *Fuel Processing Technology*, **87**(12):1095-1116. [doi:10.1016/j.fuproc.2006.08.006]

Wall, T.F., Liua, G.S., Wua, H.W., Roberts, D.G., Benfell, K.E., Guptaa, S., Lucas, J.A., Harris, D.J., 2002. The effects of pressure on coal reactions during pulverised coal combustion and gasification. *Progress in Energy and Combustion Science*, **28**(5):405-433. [doi:10.1016/S0360-1285(02)00007-2]

Wang, Q.H., Jing, N.J., Luo, Z.Y., Li, X.M., Jie, T., 2010. Experiments on the effect of chemical components of coal ash on the sintering temperature. *Journal of China Coal Society*, **35**(6):1015-1020 (in Chinese).

Wu, H.W., Bryant, G., Wall, T., 2000. The effect of pressure on ash formation during pulverized coal combustion. *Energy & Fuels*, **14**(4):745-750. [doi:10.1021/ef990080w]

Yang, J.K., Xiao, B., Boccaccini, A.R., 2009. Preparation of low melting temperature glass-ceramics from municipal waste incineration fly ash. *Fuel*, **88**(7):1275-1280. [doi:10.1016/j.fuel.2009.01.019]